REPORT DOCUMENTATION PAGE

Form Approved OMB NO. 0704-0188

1. REPORT DATE (DD-MM-YYYY)	2. REPORT TYPE	3. DATES COVERED (From - To)
	New Reprint	-

4. TITLE AND SUBTITLE
High performance multiwall carbon nanotube bolometers

5a. CONTRACT NUMBER
W911NF-09-1-0295

5b. GRANT NUMBER

5c. PROGRAM ELEMENT NUMBER
611102

6. AUTHORS
Rongtao Lu, Jack Shi, Javier Baca, Judy Wu

5d. PROJECT NUMBER

5e. TASK NUMBER

5f. WORK UNIT NUMBER

7. PERFORMING ORGANIZATION NAMES AND ADDRESSES
University of Kansas Center for Research, Inc.
2385 Irving Hill Road

Lawrence, KS 66045 -7568

8. PERFORMING ORGANIZATION REPORT NUMBER

9. SPONSORING/MONITORING AGENCY NAME(S) AND ADDRESS(ES)
U.S. Army Research Office
P.O. Box 12211
Research Triangle Park, NC 27709-2211

10. SPONSOR/MONITOR'S ACRONYM(S)
ARO

11. SPONSOR/MONITOR'S REPORT NUMBER(S)
56050-EL.14

12. DISTRIBUTION AVAILIBILITY STATEMENT
Approved for public release; distribution is unlimited.

13. SUPPLEMENTARY NOTES
The views, opinions and/or findings contained in this report are those of the author(s) and should not contrued as an official Department of the Army position, policy or decision, unless so designated by other documentation.

14. ABSTRACT
High infrared bolometric photoresponse has been observed in multiwall carbon nanotube □MWCNT□ films at room temperature. The observed detectivity D□ in exceeding 3.3 □106 cm Hz1/2 /W on MWCNT film bolometers is a factor of 7 higher than that obtained on the single-wall CNT □SWCNT□ counterparts. The response time of about 1–2 ms on MWCNT bolometers is more than an order of magnitude shorter than that of SWCNT bolometers. The

15. SUBJECT TERMS
carbon nanotube, infrared detector, bolometer

16. SECURITY CLASSIFICATION OF:			17. LIMITATION OF ABSTRACT	15. NUMBER OF PAGES	19a. NAME OF RESPONSIBLE PERSON
a. REPORT	b. ABSTRACT	c. THIS PAGE			Judy Wu
UU	UU	UU	UU		19b. TELEPHONE NUMBER: 785-864-3240

Standard Form 298 (Rev 8/98)
Prescribed by ANSI Std. Z39.18

Report Title

High performance multiwall carbon nanotube bolometers

ABSTRACT

High infrared bolometric photoresponse has been observed in multiwall carbon nanotube □MWCNT□ films at room temperature. The observed detectivity D□ in exceeding 3.3 □106 cm Hz1/2 /W on MWCNT film bolometers is a factor of 7 higher than that obtained on the single-wall CNT □SWCNT□ counterparts. The response time of about 1–2 ms on MWCNT bolometers is more than an order of magnitude shorter than that of SWCNT bolometers. The observed high performance may be attributed to the naturally suspended inner-shell structure in a MWCNT, which enhances photon absorption and restricts bolometer external thermal link to environment. © 2010 American Institute of Physics

REPORT DOCUMENTATION PAGE (SF298)
(Continuation Sheet)

Continuation for Block 13

ARO Report Number 56050.14-EL
High performance multiwall carbon nanotube bo ...

Block 13: Supplementary Note

Approved for public release; distribution is unlimited.

High performance multiwall carbon nanotube bolometers

Rongtao Lu,[1,a)] Jack J. Shi,[1] F. Javier Baca,[1,2] and Judy Z. Wu[1]
[1]*Department of Physics and Astronomy, University of Kansas, Lawrence, Kansas 66045, USA*
[2]*MPA-STC, Los Alamos National Laboratory, MS K673, Los Alamos, New Mexico 87545, USA*

(Received 15 June 2010; accepted 14 August 2010; published online 21 October 2010)

High infrared bolometric photoresponse has been observed in multiwall carbon nanotube (MWCNT) films at room temperature. The observed detectivity D^* in exceeding 3.3×10^6 cm $Hz^{1/2}/W$ on MWCNT film bolometers is a factor of 7 higher than that obtained on the single-wall CNT (SWCNT) counterparts. The response time of about 1–2 ms on MWCNT bolometers is more than an order of magnitude shorter than that of SWCNT bolometers. The observed high performance may be attributed to the naturally suspended inner-shell structure in a MWCNT, which enhances photon absorption and restricts bolometer external thermal link to environment. © *2010 American Institute of Physics*. [doi:10.1063/1.3492633]

I. INTRODUCTION

Over the past decade or so, extensive efforts have been put forth to explore device applications of carbon nanotube (CNT). CNT based infrared (IR) detectors, especially those with single-wall CNTs (SWCNTs),[1–4] have received much attention due to their moderate band gap of ~0.4–2.0 eV (Refs. 5 and 6) and high absorption efficiency in IR band.[7] The observed photoresponse under IR radiation has been argued to be dominantly bolometric effect via exciton generation and dissociation.[2,8] This is in contrast to the direct photoconductivity possibly due to transition associated to the series of van Hove singularity in one-dimensional electronic density states.[9,10] The bolometric effect may not be observable if the CNT's thermal link to the environment is sufficiently high. Considering a high thermal conductance of up to 8000 W/mK at room temperature reported for individual SWCNT,[11] reducing the CNT film's thermal link to the environment is thus necessary in order to obtain an adequate bolometric photoresponse.[2,3,12,13]

One way to reduce the thermal link is to suspend SWCNT films and enhanced bolometric photoresponse has been obtained.[2,3] Nevertheless, the best-obtained bolometer detectivity (D^*) around 4.5×10^5 cm $Hz^{1/2}/W^3$ is nearly three orders of magnitude lower than that of conventional VO_x bolometers.[14] In addition, the response time of the SWCNT film bolometers in the range of 40–60 ms must be further reduced by at least a factor of 5–10 for practical applications of IR imaging systems.[12,13,15] Further improvement of SWCNT bolometer performance faces several fundamental limitations associated with the SWCNT films including reduced light absorption at small thickness approaching percolation threshold, difficulties in suspending very thin CNT films, a large number of intertube junctions that may limit electrical and thermal transport, and a large surface area that amplifies effects of molecules such as oxygen attached to CNT surface.[16,17]

Multiwall CNTs (MWCNTs) may provide a unique solution to address these performance limitations. A MWCNT can be viewed as a set of coaxial graphene cylinders with fixed intershell spacing of ~0.34 nm.[5] This could lead to an enhanced light absorption per tube and the enhancement is proportional to the number of inner shells. In addition, all inner CNT shells are naturally suspended in MWCNTs, which is a desired configuration for optimal bolometeric photoresponse.[2,3] In MWCNTs, the neighboring shells are incommensurate, prohibiting charge delocalization in the radial direction and results in highly anisotropic charge and thermal conduction between the axial (higher conduction) and radial (lower conduction) directions.[18,19] In a transport study on MWCNTs with electrodes directly on the sidewall of the MWCNT, it has been found that the outmost shell (or few shells) of the MWCNT, which could be either semiconducting or metallic, plays the dominant role in electrical and thermal transport considering electrodes are typically laid on the outmost shell.[19] This means that the phonons generated on the inner shells of a MWCNT via photon absorption and exciton dissociation can only be dissipated after reaching the outmost shell. The semiconductor band gap of MWCNTs decreases approximately inversely with the tube diameter, making MWCNT a promising material for IR detection in the entire IR band. Motivated by these advantages of MWCNTs, we have investigated IR photoresponse of suspended and unsuspended MWCNT films with comparison also made with their SWCNT counterparts. Significant enhancement of the IR photoresponse and reduction in the response time have been observed in MWCNT films. The fitting of the observed photoresponse of MWCNT films with a bolometer model confirmed that the observed photoresponse is primarily bolometric. MWCNT is therefore indeed a promising candidate for IR nanobolometers with high sensitivity and fast response. In this paper, we report our results.

II. EXPERIMENTAL DETAILS

CNT films were prepared in a vacuum filtration process using SWCNTs and MWCNTs synthesized via chemical vapor deposition (Shenzhen Bill Technology Development Ltd., China).[3,20] The diameter of SWCNT is typically less than 2 nm while that of the MWCNT is around 40–60 nm.

a)Electronic mail: rtlu@ku.edu.

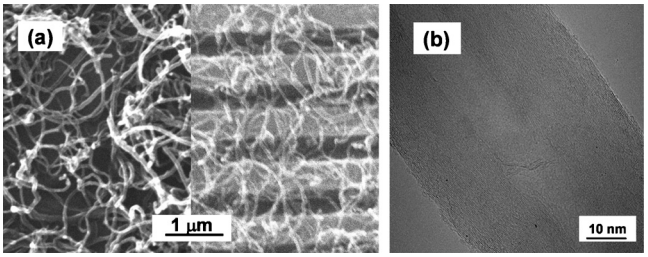

FIG. 1. (a) SEM images of unsuspended (left) and suspended (right) MWCNT films. (b) A TEM image of a representative MWCNT. The shell number is estimated to be ~40–50 for the MWCNTs used in this experiment.

The unsuspended CNT films were transferred onto SiO_2/Si (001) substrates with 500 nm thick thermal oxide layer. Parallel channels were defined using electron beam lithography (EBL) before CNT film transfer on the same type of substrates for suspending CNT films.[3] The channel width and channel spacing are both around 0.5 μm. The overall EBL patterned area was about 270×270 μm^2. The average film thickness of SWCNT films was estimated to be about 80 nm using a KLA Tencor P-16 profiler. MWCNT films are not continuous and the average thickness was estimated to be 100–200 nm. Suspension of MWCNT film thinner than this thickness is difficult due to serious film deformation. Several samples were studied for each kind for consistency. The same electrode configuration was used for both suspended and unsuspended CNT films. Four Au(25 nm)/Ti(5 nm) electrodes were deposited on all substrates for four-probe transport measurements. The voltage electrodes spacing is about 0.35 mm and the width of all CNT films was about 0.3–0.4 mm. Thermal annealing of CNT films was made in vacuum of $<5\times10^{-6}$ Torr at 400 °C for 90 min. The improvement of the temperature coefficient of resistance (TCR) on both SWCNT (Ref. 20) and MWCNT (this work) after annealing was attributed to an enhanced intertube coupling. IR radiation was provided by a xenon flash light (Stinger 75014, Streamlight, Inc.) with a near IR filter (X-Nite1000C, LDP LLC; 1000 nm cutoff at 50%, 1300 nm passband >90%). IR power intensity was calibrated using a Thorlabs PM100D thermal powermeter. Noise property was examined using a SR760 spectrum analyzer. All measurements were performed in air at room temperature.

III. RESULTS AND DISCUSSIONS

Figure 1(a) shows scanning electron microscopy (SEM) images of representative MWCNT films in the unsuspended (left) and suspended (right) forms, respectively. Unlike their SWCNT counterparts,[3] the MWCNT films contain substantial uncovered substrate areas. This means the labeled thickness of MWCNT films has a large uncertainty. In addition, some minor deformation of recess is visible on suspended MWCNT films, which is similar to the SWCNT film case in the same thickness range.[3] Figure 1(b) includes a transmission electron microscopy (TEM) image of a representative individual MWCNT, which has a large hollow center of approximately 10–11 nm in diameter and contains approximately 40–50 CNT shells.

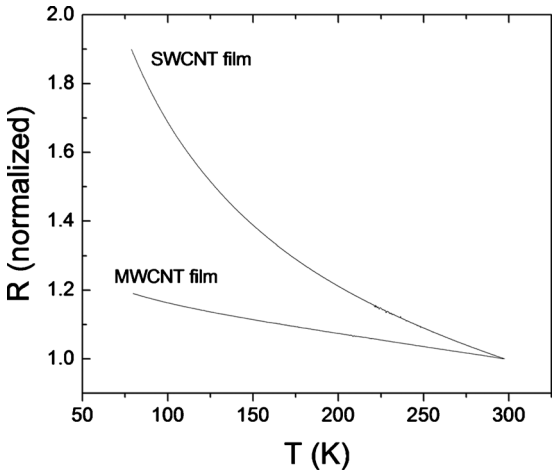

FIG. 2. Resistance vs temperatures curves of SWCNT films and MWCNT films.

All MWCNT films studied in this work show semiconductive resistance-temperature (R-T) behaviors and a representative curves is depicted in Fig. 2. Nevertheless, the increase in the resistivity of MWCNT films is much less than that of SWCNT films with decreasing temperature, as shown in Fig. 2. This is not unexpected considering a much smaller band gap in MWCNTs. The reduced temperature dependence also implies smaller TCR absolute value in MWCNTs. For example, the TCR absolute value at room temperature for MWCNT films is about 0.07%/K in contrast to ~0.17%/K for SWCNT films. R-T curve after suspending the MWCNT film has been also measured (not shown) and the room temperature TCR remains the same as before suspending.

Figure 3 compares the photoresponse R/R_0 of MWCNT films in unsuspended (a) and suspended (b) cases, where R_0 is the sample resistance before IR radiation was turned on and the change in the resistance caused by IR radiation is defined as $\Delta R=R-R_0$. For comparison, the results of their SWCNT counterparts are also included in Fig. 3(c) (unsuspended) and Fig. 3(d) (suspended). Two major differences are visible between MWCNT and SWCNT films, a significantly higher $\Delta R/R_0$ and a much shorter response time in the cases of MWCNT. The $\Delta R/R_0$ for MWCNT samples is typically in the range of a few percents, which is more than one order of magnitude higher than that of suspended SWCNT films and two orders of magnitude higher than the unsuspended SWCNT films at a comparable IR power. Considering a lower TCR absolute value in MWCNTs, the much enhanced photoresponse of MWCNT films should be attributed to the naturally suspended inner CNT shells, which may provide an ideal configuration to enhance the bolometric effect by improving light absorption and reducing thermal link. Physical suspension of the films in both MWCNT [Fig. 3(b)] and SWCNT [Fig. 3(d)] cases results in a further improvement of $\Delta R/R_0$ as compared to their unsuspended counterparts. The improvement is, however, much more pronounced (by a factor of 5–10) in SWCNT film than in MWCNT film (by a factor of 2). Considering the same physical suspension structures employed for both SWCNT and MWCNT films, it is plausible to argue that the proportions of the reduction in direct thermal link to substrate are comparable in the two

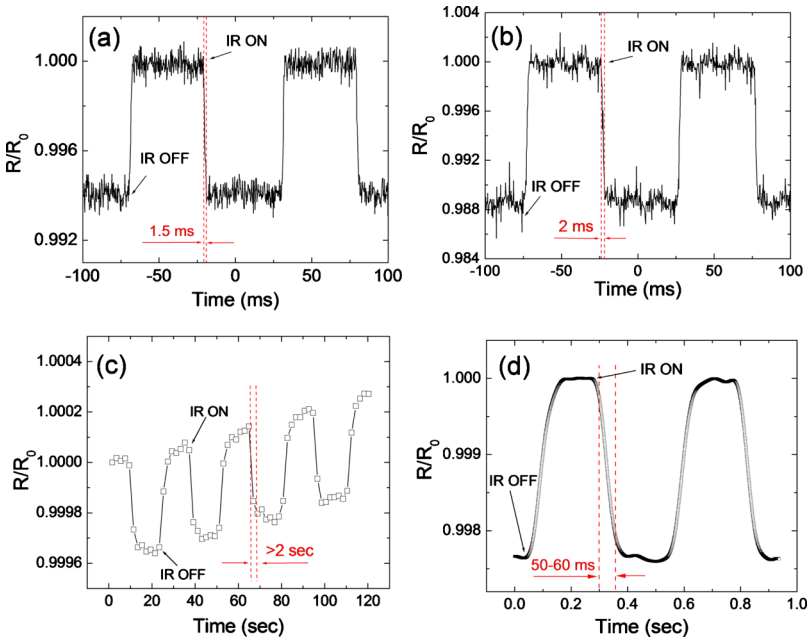

FIG. 3. (Color online) Photoresponse of unsuspended and suspended CNT films. (a) Unsuspended MWCNT film, f=10 Hz, in IR~3 mW/mm^2; (b) suspended MWCNT film, f=10 Hz, in IR~3 mW/mm^2; (c) unsuspended SWCNT film, f=1/30 Hz, in IR ~3.5 mW/mm^2; and (d) suspended SWCNT film, f =2 Hz, in IR~3.5 mW/mm^2.

suspended cases. The much greater improvement of $\Delta R/R_0$ by suspending SWCNT films therefore suggests the $\Delta R/R_0$ in unsuspended SWCNT film may contain a considerable portion of nonbolometric photoresponse, such as direct photoconductivity. The direct photoconductivity in SWCNT is fairly weak even under high intensity laser. The possible electron plasmon excitation[16] may facilitate electron transfer to molecules attached to the CNT surface, leading to a rather large relaxation time (response time) on the order of several seconds.[1] The low photoresponse and large response time observed on unsuspended SWCNT film are consistent to these characteristic features. However, direct photoconductivity may not play a significant role in unsuspended MWCNT films in which the bolometric response is significantly enhanced by naturally suspending CNT inner shells.

The other major difference between MWCNT and SWCNT films is in much shorter response time in the former case. For MWCNT films, the response time is in the range of 1.0–2.6 ms. Here the response time was measured from 10% to 90% magnitude change in $\Delta R/R_0$ with 10 Hz modulation (chopping) of the incident IR radiation. This is a significant improvement on the response time of 40–60 ms of the suspended SWCNT films and several seconds for the unsuspended SWCNT films.

To better understand the observed IR photoresponse of CNT films, the measured photoresponse was compared with the theoretical calculation based on the bolometric heat balance equation with the measured R-T curve and the temperature dependence of the specific heat of the films. The bolometric heat balance equation with a constant bias current can be written as[12]

$$mC\frac{dT}{dt} = \eta PH(t) + I^2R - G(T - T_0), \tag{1}$$

where T and T_0 are the film and heat sink temperatures, respectively, m and C are the mass and specific heat of the film, η is the radiation absorbance of the film, P is the incident radiation power, I is the bias current, R is the resistance of the film, G is the total thermal conduction coefficient, and H(t) is a rectangular pulse with H(t)=1 when the incident radiation is on and H(t)=0 when the incident radiation is off. The heat sink temperature is assumed to be the same as the ambient temperature, i.e., $T_0 \simeq 300$ K for the case of this experiment. Note that the linear T-dependence term of the thermal energy loss due to the blackbody radiation of the film is included in the term of G and the higher-order terms of the energy loss were neglected in Eq. (1). The T-dependence of R was obtained by fitting the measured R-T curves in Fig. 2. For SWCNT films, the temperature increase ΔT of the photoresponse is much smaller than T_0 and, therefore, only the linear term of the T-dependences of R is needed here, i.e.,

$$\frac{\Delta R}{R_0} = \frac{R - R_0}{R_0} \cong -\alpha\frac{\Delta T}{T_0}, \tag{2}$$

where $R_0=R(T_0)$ and $\alpha \simeq 0.48$ at $T_0=300$ K. For MWCNT films, the fitting of the measured R-T curve near T_0 =300 K yields a similar linear T-dependence but $\alpha \simeq 0.23$. For the T-dependence of C, the published data was used.[21–23] Near $T_0=300$ K, it can be approximated for both SWCNT and MWCNT that

$$C(T) \simeq C_0 + C_1(T - T_0), \tag{3}$$

where $C_0 \simeq 650$ J/(kg K) and $C_1 \simeq 2.0$ J/(kg K^2) for SWCNT while $C_0 \simeq 450$ J/(kg K) and $C_1 \simeq 1.5$ J/(kg K^2) for MWCNT. With Eqs. (2) and (3), the dynamics of the bolometric response can be solved from Eq. (1). In this experiment, the modulation period of the incident radiation is much larger than the response time of the photoresponse (see Fig. 3). In this situation, the photoresponse has enough time to reach its maximal temperature change (steady state) and follows the rectangular pulse of the incident radiation. This maximal temperature change obtained from Eq. (1) is then

$$\left(\frac{\Delta T}{T_0}\right)_{max} = \frac{\eta P + I^2 R_0}{G T_0 + \alpha I^2 R_0}, \quad (4)$$

and the response time can be written as

$$\tau_s = a_1 \left[a_2 + \left(\frac{\Delta T}{T_0}\right)_{max} \right] \left(\frac{\Delta T}{T_0}\right)_{max}, \quad (5)$$

where $a_1 = mC_1T_0/(\eta P + I^2R_0)$ and $a_2 = C_0/(C_1T_0)$. Note that the values of a_1 and a_2 do not depend on whether a CNT film is unsuspended or suspended. The suspension of a CNT film only reduces the thermal conduction G. Let γ_{su} and γ_{un} be the maximum values of $(\Delta T/T_0)_{max}$ of a suspended and unsuspended CNT films while τ_{su} and τ_{un} are the response time of the suspended and unsuspended films, respectively. If a pair of unsuspended and suspended CNT films have otherwise similar physical characteristics, which is the case of this experiment, the ratio of their time constants is then

$$\frac{\tau_{su}}{\tau_{un}} \simeq \frac{(a_2 + \gamma_{su})\gamma_{su}}{(a_2 + \gamma_{un})\gamma_{un}}. \quad (6)$$

This scaling relationship can be conveniently used to verify the bolometric effect of a CNT film by comparing the measured photoresponses between a suspended and unsuspended film.

In the case of MWCNT, we have $\gamma_{su} \simeq 0.052$ extracted from Fig. 3(b) and $\gamma_{un} \simeq 0.026$ from Fig. 3(a). Based on the measured specific heat,[21] $a_2 \simeq 1$ for MWCNT. The ratio of the response time between the suspended and unsuspended MWCNT films calculated from Eq. (6) is then $\tau_{su}/\tau_{un} \simeq 2.0$. On the other hand, the value of this ratio directly calculated with the measured response time from Figs. 3(a) and 3(b) is around 1.3. The observed photoresponses on the MWCNT films therefore qualitatively agree with the model, which confirms that the observed photoresponse of MWCNT films is dominantly a bolometric effect and a reduction in the thermal link in suspended MWCNT films leads to a smaller G and therefore longer response time.

In the case of SWCNT, the maximal photoresponses in Figs. 3(c) and 3(d) are $\gamma_{un} \simeq 0.8 \times 10^{-3}$ and $\gamma_{su} \simeq 0.5 \times 10^{-2}$, respectively. From the measured specific heat of SWCNT,[22,23] $a_2 \gg \gamma_{su}$. The ratio of the response time calculated from Eq. (6) is then $\tau_{su}/\tau_{un} \simeq 6.3$. A direct calculation of τ_{su} and τ_{un} from Figs. 3(c) and 3(d), however, suggests that $\tau_{su}/\tau_{un} \ll 1$. The observed photoresponse in SWCNT films is therefore inconsistent with the bolometer model. Note that the response time of a bolometer is the consequence of the thermal dissipation and is inversely proportional to the thermal conduction. Since the suspension of the film reduces the thermal conduction, the increase in the photoresponse after the suspension is agreeable with bolometric effect being dominant. The photoresponse of the unsuspended SWCNT film is therefore most probably not a bolometric effect, which may be affected by the large surface area and massive intertube junctions inherent to SWCNT films.

A question arises on why much enhanced bolometric photoresponse is observed on unsuspended MWCNT films as compared to their SWCNT counterparts. Although a complete answer requires a systematic investigation of the photoresponse, this study reveals a critical effect of the microscopic configuration of CNTs to the photoresponse. The naturally suspended CNT inner-shell configuration in a MWCNT may provide several favorable effects to enhanced bolometric photoresponse including high radiation absorbance per tube, engineered thermal link to environment, reduced surface area and intertube junctions.

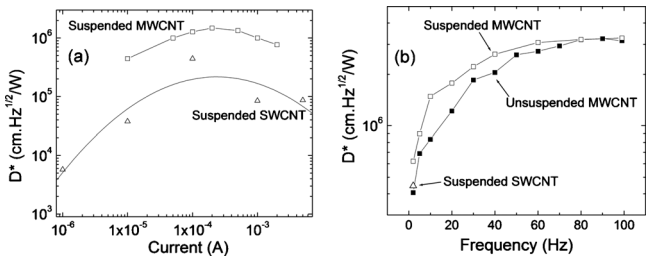

FIG. 4. (a) D^* as function of bias current I for suspended MWCNT (square) and SWCNT (triangle) films. The modulation frequencies were 10 Hz for MWCNT and 2 Hz for SWCNT films. (b) D^* as function of modulation frequency for MWCNT films. Solid squares: unsuspended MWCNT film, I=2 mA; open squares: suspended MWCNT film, I=200 μA. The open triangle in (b) shows the D^* of suspended SWCNT film at f=2 Hz. The IR intensity of 0.3 mW/mm^2 was applied in all measurements.

Figure 4(a) plots the detectivity as a function of the bias current I for the suspended MWCNT and SWCNT films. The detectivity is defined as $D^* = R_V\sqrt{A_d}/V_n$,[12] where A_d is the active detection area, V_n is the root-mean-square noise voltage per unit bandwidth, and $R_V = \Delta V/\Delta P$ is the responsivity that is defined as the ratio of the voltage change (ΔV) and the power (ΔP) of incident IR radiation. The modulation frequencies of the incident radiation were 10 Hz for MWCNT films and 2 Hz for SWCNT films, respectively. The D^*-I curves show a qualitatively similar parabola shape for both MWCNT and SWCNT films, which is similar to that reported in traditional VO_x uncooled IR bolometers,[14,24] The D^* peak of the suspended MWCNT film (square) is $\sim 1.5 \times 10^6$ cm Hz$^{1/2}$/W, which is more that three times higher than the peak $D^* \sim 4.5 \times 10^5$ cm Hz$^{1/2}$/W for the suspended SWCNT film (triangle). This improved D^* is a consequence of the naturally suspended multishell structure of MWCNT, as discussed above. A similar variation trend was also observed on unsuspended MWCNT film (not shown) with a peak $D^* \sim 8.3 \times 10^5$ cm Hz$^{1/2}$/W. For CNT, the major noise has been reported to be 1/f noise at low frequencies.[25–27] The V_n is expected to increase with bias current at a fixed frequency, which has been confirmed experimentally. The parabola shape of the D^* versus current curves is attributed to self heating and TCR decrease at higher dc bias current in VO_x bolometers.[14,24] At higher current the self heating leads to R_V drifting downwards from the linear I-dependence, causing D^* decreasing after reaching a peak at certain bias current. In both suspended and unsuspended CNT films the R_v indeed shift downwards from the linear R_v versus I curves at higher bias, indicating a similar mechanism to that in VO_x bolometers. In the unsuspended MWCNT film case the peak D^* appears at much higher bias current, this might be induced by the reduced self-heating with improved thermal link to environment.

The frequency dependence of D^* at IR power intensity

of 0.3 mW/mm^2 is depicted in Fig. 4(b) for both suspended and unsuspended MWCNT films. It should be pointed out that this curve can not be obtained on suspended SWCNT films due to the limitation of large response time, thus only one point (open triangle) was added to represent the D^* of suspended SWCNT film at 2 Hz. The curves for suspended/unsuspended MWCNT films show a same trend that D^* increases monotonically with f at lower frequencies, which is expected as a consequence of monotonically decreasing $V_n \propto 1/f^{1/2}$ and weak frequency dependence of R_v. This variation is consistent with previously reported results in conventional vanadium oxide based bolometers.[28] Since 1/f noise dominates the noise spectrum at low frequencies below the corner frequency, V_n is expected to saturate at the thermal noise when frequency is higher than the corner frequency.[25–27] On the other hand, R_v decreases very slowly with increasing frequency due to the small response time, the D^* is expected to eventually saturate at a certain value when V_n almost reaches its saturation at near the corner frequency. Despite a slightly lower D^* for unsuspended MWCNT film, a maximum value of about 3.3×10^6 cm $Hz^{1/2}/W$ was observed for both suspended and unsuspended MWCNT samples at around 80–90 Hz. The comparable performance of D^* and response time in suspended and unsuspended MWCNT films suggests the natural suspension of inner CNT shells plays a dominant role in enhancing the bolometric photoresponse. Moreover, the saturated high D^* value on MWCNT films is more than seven times of the best D^* of 4.5×10^5 cm $Hz^{1/2}/W$ [open triangle] so far achieved on suspended SWCNT film bolometer,[3] which further confirms the advantage of MWCNT film for bolometer applications.

IV. CONCLUSIONS

In conclusion, the naturally suspended inner CNT shells structure in MWCNT provides a unique microscopic configuration desired for a nanoscale bolometer with high photon absorption and engineered thermal conduction. Significantly improved IR photoresponse, fast response time, and high bolometer detectivity have been observed in both suspended and unsuspended MWCNT films as compared to their SWCNT counterparts. The observed high detectivity D^* and short response time around 1–2 ms represent the best so far achieved on CNT film bolometers. These results suggest MWCNT film based IR bolometers may become competitive for practical application of uncooled IR detection with further optimization.

ACKNOWLEDGMENTS

This research was supported by ARO (ARO-W911NF-09-1-0295). J.W. also acknowledges support from NSF (NSF-DMR-0803149).

[1] I. A. Levitsky and W. B. Euler, Appl. Phys. Lett. **83**, 1857 (2003).
[2] M. E. Itkis, F. Borondics, A. P. Yu, and R. C. Haddon, Science **312**, 413 (2006).
[3] R. T. Lu, Z. Z. Li, G. W. Xu, and J. Z. Wu, Appl. Phys. Lett. **94**, 163110 (2009).
[4] F. B. Rao, X. Liu, T. Li, Y. X. Zhou, and Y. L. Wang, Nanotechnology **20**, 055501 (2009).
[5] M. Dresselhaus, G. Dresselhaus, and P. Avouris, *Carbon Nanotubes: Synthesis, Structure, Properties and Applications* (Springer, Berlin, 2001).
[6] J. W. G. Wildoer, L. C. Venema, A. G. Rinzler, R. E. Smalley, and C. Dekker, Nature (London) **391**, 59 (1998).
[7] M. E. Itkis, S. Niyogi, M. E. Meng, M. A. Hamon, H. Hu, and R. C. Haddon, Nano Lett. **2**, 155 (2002).
[8] F. Wang, G. Dukovic, L. E. Brus, and T. F. Heinz, Science **308**, 838 (2005).
[9] A. Mohite, S. Chakraborty, P. Gopinath, G. U. Sumanasekera, and B. W. Alphenaar, Appl. Phys. Lett. **86**, 061114 (2005).
[10] S. X. Lu and B. Panchapakesan, Nanotechnology **17**, 1843 (2006).
[11] C. H. Yu, L. Shi, Z. Yao, D. Y. Li, and A. Majumdar, Nano Lett. **5**, 1842 (2005).
[12] E. L. Dereniak and G. D. Boreman, *Infrared Detectors and Systems* (Wiley, New York, USA, 1996).
[13] A. Rogalski, *Infrared Detectors* (Gordon & Breach, Amsterdam, 2000).
[14] C. H. Chen, X. J. Yi, X. R. Zhao, and B. F. Xiong, Sens. Actuator A, Phys. **90**, 212 (2001).
[15] A. Wood, *Uncooled Infrared Imaging Array and Systems* (Academic, New York, 1997).
[16] R. J. Chen, N. R. Franklin, J. Kong, J. Cao, T. W. Tombler, Y. G. Zhang, and H. J. Dai, Appl. Phys. Lett. **79**, 2258 (2001).
[17] P. G. Collins, K. Bradley, M. Ishigami, and A. Zettl, Science **287**, 1801 (2000).
[18] M. Fujii, X. Zhang, H. Q. Xie, H. Ago, K. Takahashi, T. Ikuta, H. Abe, and T. Shimizu, Phys. Rev. Lett. **95**, 065502 (2005).
[19] B. Bourlon, C. Miko, L. Forro, D. C. Glattli, and A. Bachtold, Phys. Rev. Lett. **93**, 176806 (2004).
[20] R. T. Lu, G. W. Xu, and J. Z. Wu, Appl. Phys. Lett. **93**, 213101 (2008).
[21] W. Yi, L. Lu, D. L. Zhang, Z. W. Pan, and S. S. Xie, Phys. Rev. B **59**, R9015 (1999).
[22] I. Hone, in *Dekker Encyclopedia of Nanoscience and Nanotechnology*, edited by J. A. Schwarz, C. I. Contescu, and K. Putyera (Dekker, New York, 2004), p. 603.
[23] S. V. Rotkin and S. Subramoney, *Applied Physics of Carbon Nanotubes* (Springer, New York, 2005).
[24] S. He, X. Wang, J. Dai, Y. Huang, J. Lai, and X. Yi, Proceedings of the Seventh IEEE International Conference on Nanotechnology, Hong Kong, 2–5 August 2007, p. 1269.
[25] H. Ouacha, M. Willander, H. Y. Yu, Y. W. Park, M. S. Kabir, S. H. M. Persson, L. B. Kish, and A. Ouacha, Appl. Phys. Lett. **80**, 1055 (2002).
[26] W.-J. Kong, L. Lü, D.-L. Zhang, and Z.-W. Pan, Chin. Phys. **14**, 2090 (2005).
[27] B. Lassagne, B. Raquet, J. M. Broto, J. P. Cleuziou, T. Ondarcuhu, M. Monthioux, and A. Magrez, New J. Phys. **8**, 31 (2006).
[28] Y. H. Han, K. T. Kim, H. J. Shin, S. Moon, and I. H. Choi, Appl. Phys. Lett. **86**, 254101 (2005).